

Nitriding of steel 40x with a high-intensity ion beam

A I Ryabchikov, Tran My Kim An, T V Koval, D O Sivin, P S Anan'in, O S Korneva

National Research Tomsk Polytechnic University, 30 Lenin Ave., Tomsk, 634050, Russia

E-mail: tvkoval@mail.ru

Abstract. The results of experimental and theoretical studies of the regularities and features of the modification of steel 40X with high-intensity beams of low-energy nitrogen ions are provided. The study of the effect of high-intensity, ultra-high-fluency implantation of low-energy nitrogen ions at temperatures of steel 40X samples in the range of 450-650 °C are presented. It is established, that the width of the nitrided layer, during 60 minutes, depends both on the temperature implantation regime and on the ion current density, the maximum depth of nitrogen penetration of 180 μm was observed at a target treatment temperature of 500 °C. The results of numerical simulation agree with the experiments and allow predicting the structure of surface layers when the geometry of the system and parameters of a high-intensity low-energy beam of nitrogen ions change.

1. Introduction

Nitriding is one of the most effective methods of surface hardening of tool materials which improves hardness and wear resistance, corrosion resistance [1, 2]. The works [3, 4] showed with an increase in an ion current density up to 5-10 mA/cm², a nitrogen dopant penetration depth into the surface of the workpiece during implantation of low energy nitrogen ions increases. Ion energy ceases to be a parameter at high-intensity ion implantation and surface sputtering by an ion beam becomes a dominant process resulting in doped layer decrease, the upper range of the implanted dopant is limited to 20–50 at.% [3, 5].

The possibility of plasma-immersion formation of high-intensity repetitively-pulsed beams of low-energy ions with a current density of 10⁻²-1 A/cm² was first shown in work [6].

At high-intensity pulse nitrogen implantation in the workpiece surface layer, processes of radiation-stimulated diffusion are developed, providing high speed and saturation depth (~10-150 μm). At high-intensity nitrogen implantation, nitrides can exist as a solid solution and remain in a free state located in defects, cracks [5]. The depth of nitration is controlled by diffusion mobility and depends on the dose and duration of processing time, temperature of the sample surface. Elastic stresses arising in the implanted layer can also be the reasons for the radiation-accelerated deep transfer of atoms inserted during ion implantation [7]. Because of the universality of the parameters that affect the growth kinetics of layers, it is difficult to create a model that includes all the important factors of the kinetics and, consequently, the formation of composite layers. Fe-N system has an ideal condition to form phases [8, 9].

This work is aimed at experimental and theoretical research of deep ion-modified layer formation of 40X structural steel using a high-intensity repetitively-pulsed low-energy nitrogen ion beam.



2. Experimental installation and research technique

Ion nitrogen implantation was carried out on an experimental installation equipped with a turbomolecular pump at a residual atmosphere pressure of 10^{-3} Pa. The installation is equipped with an arc source of a gas-discharged plasma with a hot cathode [10]. The gas-discharged plasma source functions when nitrogen is pumped into the working chamber up to pressure of 0.6 Pa and at arc discharge current of 25 A. The formation of high-intensity fluxes of low-energy nitrogen ions was performed by the plasma-immersion ion extraction method with subsequent ballistic focusing. The ion source with the focusing system was located opposite the plasma generator at a distance of 10 cm.

As model samples for nitriding, disks of 40X steel with a diameter of 20 mm and a thickness of 4 mm were used.

The target was heated by ion beam energy, and the specific temperature irradiation regime of 450 °C to 650 °C was established by the selection of a removable radiator. In all ion-target treatment regimes, ion implantation time was 60 min. All ion treatment regimes further included preheating of the target with an ion beam for at least 20 minutes.

3. High-intensity nitrogen ion beam formation

The scheme of the ion source is shown in figure 1. To form high-intensity nitrogen ion beams, the combined method was used. It was first proposed and described in [6]. The method is based on plasma-immersion extraction of ions from free plasma boundary, their acceleration in a high-voltage sheath and a beam formation with high current density by ballistic ions focusing on a target in the equipotential space of a potential electrode.

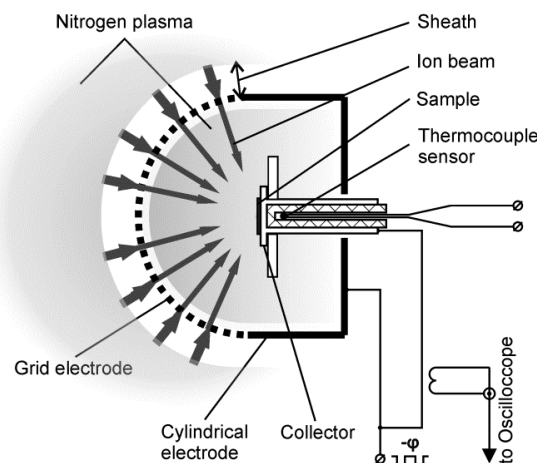


Figure 1. Scheme of the ion source.

A metal grid electrode as a part of the sphere (figure 1) with a curvature radius of 7.5 cm, with a cell size of 1.8×1.8 mm² and a transparency of 70 % was used to form a high-density nitrogen ion beam. The electrode was placed along the axis of the system at a distance of 10 cm from the output of the gas-discharged plasma generator. Samples for irradiation were placed at a distance of 7.5 cm from a grid electrode. The grid electrode and the irradiated samples were connected to a high-frequency pulsed generator of a bias voltage of negative polarity. The generator provided pulse generation of a negative bias potential with an amplitude of 1.2 kV at a pulse repetition rate of 10^5 pulses/s and a pulse duration of 4 μ s. The ion current to the collector was measured by a Rogowski coil. An active voltage-ratio divider was used to measure bias voltage characteristics.

At an ion current of 0.6 A, the maximum ion current density was 0.5 A/cm². Space charge neutralization of the focused ion beam was conducted because of the plasma injection into the drift space between bias pulses and the gas ionization by the ion beam.

4. Microstructure and nitrogen concentration

High-intensity implantation of nitrogen ions with energy of 1.2 keV is characterized by significant ion surface sputtering of the target. After 80-minute treatment, a crater with the maximum depth at the centre is formed on the surface of 40X steel sample, maximum depth of which coincides with the maximum of current density distribution of an ion beam (figure 2). Distribution of the ion current density (j) and the surface cross section of the modified samples along the nitrogen ion beam cross section in the area of crater maximum depth.

Figure 3 shows concentration profiles of nitrogen dopant distribution along the depth in nitrated samples obtained at 450 °C, 500 °C and 580 °C. The nitrogen distribution profiles along the sample depth were measured at the centre of the sprayed crater ($r = 0$ mm) and at distances of $r = 2$ mm, 4 mm, 6 mm and 8 mm.

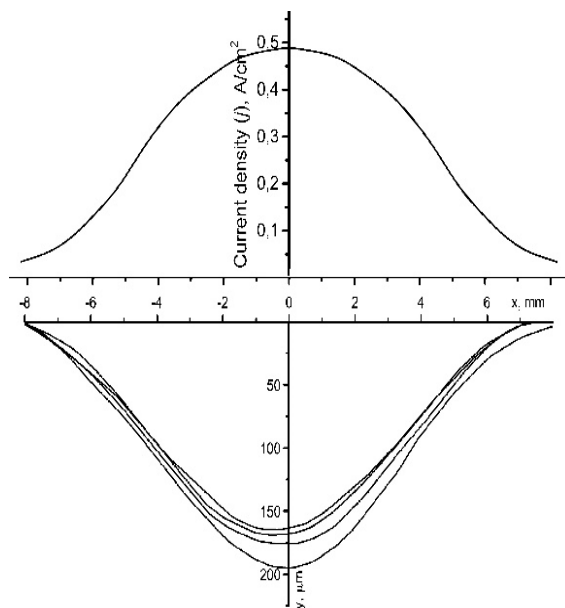


Figure 2. Distribution of the ion current density (j) and the surface cross section of the modified samples ($T = 450 \dots 650^\circ\text{C}$) along the nitrogen ion beam cross section in the area of crater maximum depth.

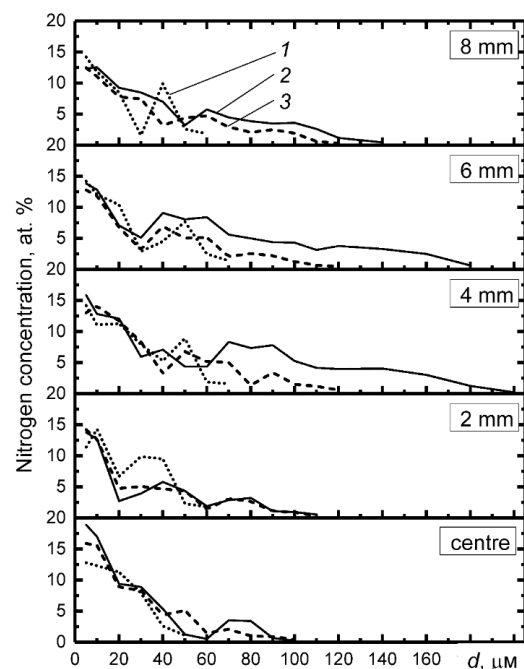


Figure 3. Concentration profiles of nitrogen dopant distribution along the depth, obtained at various distances from the centre of the sputtering crater, for samples modified at temperatures: 1 – 450°C; 2 – 500°C; 3 – 580°C.

The maximum nitrogen dopant level depth at 180 μm is observed on a sample implanted at a temperature of 500 °C. The maximum depth is observed at a distance of 4 mm from the centre at a current density in this target area of $\sim 0.3 \text{ A/cm}^2$. For a sample with a temperature of 500°C in the central area nitrogen is observed in a layer of about 100 μm thick. Simultaneously, when the distance from the crater centre increases by 6 mm and 8 mm the depth of nitrogen penetration also decreases. A less pronounced distance effect from the crater sputtering centre to a thickness of the nitrated layer was observed on the samples implanted at temperatures of 450°C and 580°C. It is characteristic that maximum thicknesses of nitrated layers in these regimes were less than 80 μm and 120 μm , respectively.

Figure 4 shows microphotographs of metallographic sections of a sample implanted at a temperature of 500°C. It is seen that in the central target area (figure 4a), the ion-modified layer width is minimal, approximately 70 μm . When the distance from the centre increases, an increase in the layer thickness with a changed structure is observed, and an explicit two-layer structure becomes apparent. The

continuous layer width at the surface is 25 μm . The total width of the modified layer is 130 μm . Further increase in the distance from the crater centre demonstrates a slight decrease in the layer width to approximate values of 120 μm .

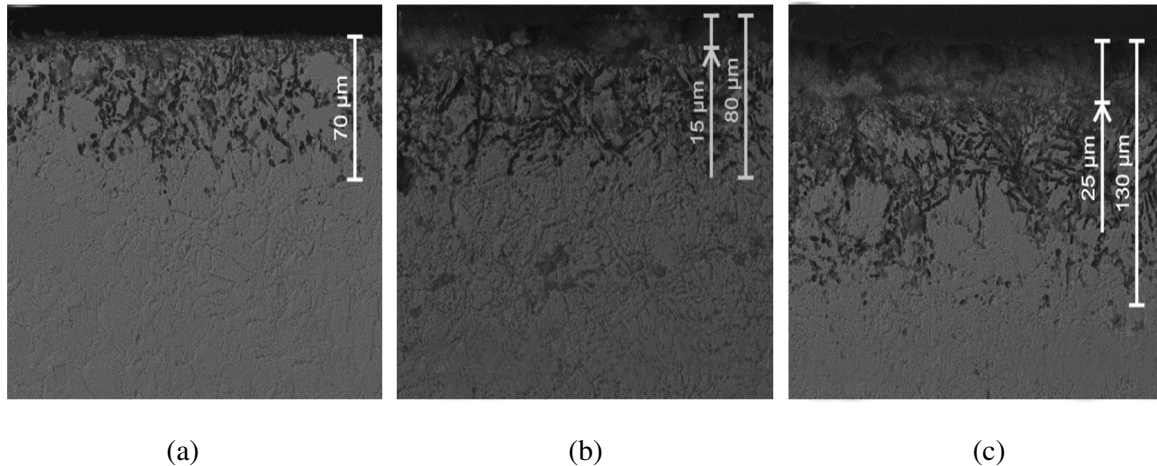


Figure 4. Microphotographs of metallographic sample sections modified at a temperature of 500°C, obtained in the centre (a) and at distances from the crater centre: b – 2 mm, c – 4 mm.

Similar structures are formed because of high-intensity ion irradiation of the target at a temperature of 450 °C. The total width of the modified layer is less than in case of irradiation at a temperature of 500 °C. The maximum thickness of the layer does not exceed 80 μm at a distance of 6 mm from the crater centre. As in the previous case, the smallest layer width is observed in the crater centre (about 50 μm). Some recession up to 75 μm occurs when the distance from the centre increases to 8 mm.

When the target temperature increases up to 580 °C, the ion-modified layer thickness decreases. The maximum layer width is 80 μm and can be observed at a distance of 4 mm to 6 mm from the crater centre. As in the previous cases of irradiation, the smallest layer thickness is observed at the target centre and is 65 μm .

5. Investigation of microhardness

Figure 6 shows the hardness dependence on the distance from the sample surface of a nitrated target layer treated at a temperature of 450°C. The dependence correlates with the study results of nitrogen concentration distribution along the depth (figure 5).

The greatest hardness of nitrated samples is observed in the near-surface layer. The maximum hardness value of 8.9 ± 0.5 GPa is observed at a depth of about 10 μm at the centre of the sputtering crater. When the depth increases to 50 μm , the hardness decreases to 4.1 ± 0.3 GPa and at a depth of 100 μm the hardness of the corresponding 40X raw steel 3.6 ± 0.3 GPa is observed. The hardness investigation at a distance from the crater centre shows a decrease in the largest value, but an increase in the area width (over 100 μm), where the hardness is higher than that of the original steel. Similar hardness dependences on the distances from the sample surface were obtained for processing temperatures of 500 °C and 580 °C. A significant change in the microhardness distribution along the depth of the ion-modified layer was observed at a temperature of 650 °C. The maximum hardness in this case did not exceed 5 GPa, and the thickness of the modified layer was at a level of 10 μm .

6. Numerical calculations

A theoretical study of deep ion-modified layer formation includes modeling of the sample heating by an ion beam and diffusion-kinetic processes in a sample with ion beam sputtering.

The mathematical model of 40X nitriding steel is constructed based on the diffusion equation with the binary phase diagram of Fe-N when the condition of conservation of mass at the boundaries between layers (compounds) is fulfilled. The dominant parameters of the process for the nitrided zone formation are time, diffusion coefficients and surface sputtering rate.

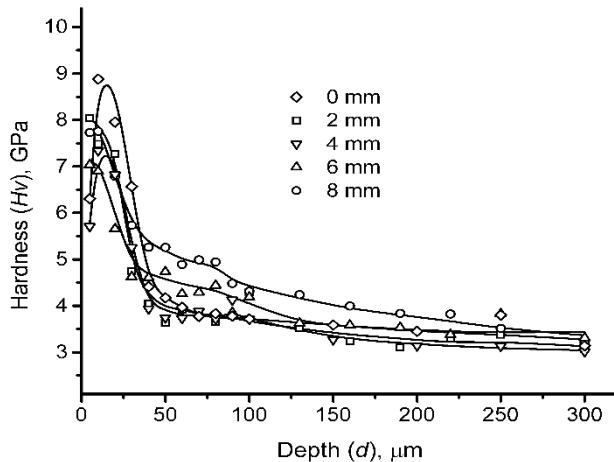


Figure 5. Dependence of the modified layer hardness (H_v) at a temperature of $450\text{ }^\circ\text{C}$ on the depth (d) at different distances from the centre of the sputtering crater: 1 – 0 mm; 1 – 4 mm; 1 – 8 mm.

The two-layer structure of the irradiated target (figure 4) indicates that in these areas the diffusion processes proceed at different rates (diffusion along grain boundaries, inside the grain). In modeling, it was considered that the first layer (width l) was formed in the saturation regime with a concentration of the lower limit of 12 at.%, and the coefficients of radiation-stimulated diffusion were estimated from the experiment results. Figure 6 shows the experimental and calculated distribution of nitrogen concentration at $T=500\text{ }^\circ\text{C}$.

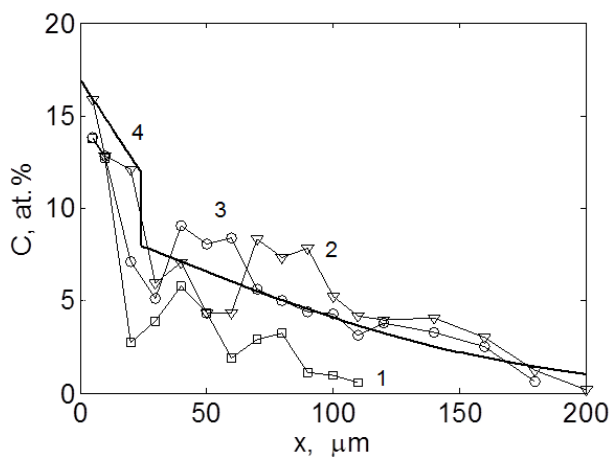


Figure 6. Experimental (1, 2, 3) and calculated (4) distribution of nitrogen concentration at $T=500\text{ }^\circ\text{C}$; 1 – $r = 0.2\text{ cm}$; 2 and 4 – 0.4 cm ; 3 – 0.6 cm .

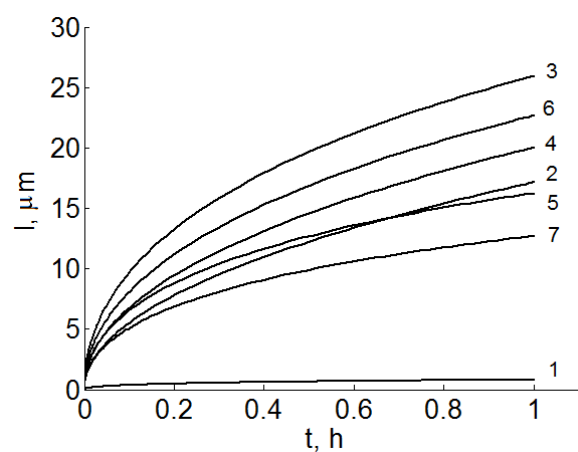


Figure 7. Change in the layer width from time: 1 – $r = 0\text{ cm}$; 2 – 0.2 cm ; 3, 6 and 7 – 0.4 cm ; 4 – 0.6 cm ; 5 – 0.8 cm ; 1,...,5 – $T=500\text{ }^\circ\text{C}$; 6 – $580\text{ }^\circ\text{C}$; 7 – $450\text{ }^\circ\text{C}$.

Figure 7 shows the dependence of the first layer width l on time at different distances from the crater centre of $r = 0, 0.2, 0.4, 0.6$ and 0.8 cm (for different values of the current density in figure 2) at a temperature of $500\text{ }^\circ\text{C}$. The temperature effect is reflected by curves 3 ($T=500\text{ }^\circ\text{C}$), 6 ($T=580\text{ }^\circ\text{C}$), and 7 ($T=450\text{ }^\circ\text{C}$) in figure 7, the optimal nitriding temperature is $500\text{ }^\circ\text{C}$. The highest rate of the first layer

growth and its width at the end of the nitriding time take place at a distance of $r = 0.4$ cm (namely at a beam current of 0.3 A/cm^2).

Increasing in the nitrided zone width when the current density varies from 50 to 300 mA/cm^2 is because of an increase in the coefficient of nitrogen radiation-stimulated diffusion. A further increase in the current density causes the formation of a surface nitrogen-containing layer, which consists of nitrides having low diffusion mobility, and prevents further saturation of the bulk layers with nitrogen. An increase in the dose rate during high-intensity nitrogen implantation leads to a decrease in the ability to form a high concentration of nitride phases, where γ' - Fe_4N is dominant [7]. The interaction of an ion beam with sputtered surface particles can also contribute to the formation of FeN nitride, which molecules are adsorbed by the surface under the effect of the incident flux directed to the surface.

With the deficiency of the first layer (figure 8) at the crater centre ($r=0$), the concentration distribution in the sample is described by the diffusion equation solution $C(x,t) = C_s \text{ierf}(x/(4Dt)^{0.5})$, nitrogen diffusion coefficient $D=10^{-13} \text{ m}^2/\text{s}$ at $T=500 \text{ }^\circ\text{C}$. The concentration value on the sample surface $C_s=18.9 \text{ at.}\%$ exceeds the minimum value ($18.3 \text{ at.}\%$) to form γ' phase (Fe_4N). The homogeneity zone of Fe_3N phase compound begins with $17 \text{ at.}\%$ [5].

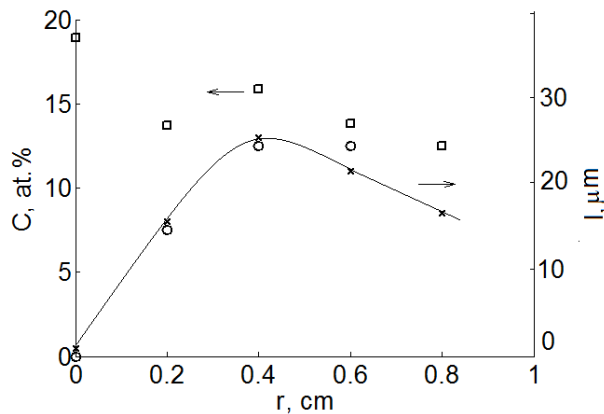


Figure 8. Change in the concentration (\square) and the layer width l from the distance to the sample centre; (\circ , \square) – experiment, ($-x-$) – calculation, $T=500 \text{ }^\circ\text{C}$.

The obtained results indicates the multifactorial effect of high-intensity implantation of low-energy nitrogen ions on the change in the elemental composition and microstructure of 40X steel layers at depths many times exceeding the ion range. Several opposing processes can be distinguished in the process of high-intensity ion irradiation. It is evident that deep ion-doped layer formation is effected by the target temperature, on which the nitrogen diffusion depends. Ion sputtering is an opposing process. The sputtered layer thickness at the target centre is commensurable and even exceeds the width of the ion-modified layer for individual irradiation regimes. It can be assumed that in case of problem solving of substantial surface sputtering by a high-intensity ion beam, for instance, by decreasing ion energy, the ion-modified layer width can be significantly increased.

7. Conclusion

The non-uniform distribution of the ion current density along the beam cross section was used to investigate the effect of ion current density of 0.1 A/cm^2 to 0.5 A/cm^2 on the crater formation by ion sputtering, nitriding depth and microstructure change and properties of modified layers on one sample for each temperature treatment regime. The effect of high-intensity, ultra-high-dose implantation of low-energy nitrogen ions at temperatures of 40X steel samples in the range from 450°C to 650°C was investigated. It was established that the nitrided layer width, within 60 minutes, depended both on the temperature implantation regime and on the ion current density. The maximum nitrogen penetration depth of $180 \mu\text{m}$ was observed at a target treatment temperature of 500°C in the area of the ion current density of 0.3 A/cm^2 . At a maximum ion current density (0.5 A/cm^2), the nitrided layer width was 44% smaller. Nitrogen implanted samples at temperatures of 450°C , 500°C , and 580°C revealed a significant increase in hardness.

Theoretical studies have shown that 40X steel nitriding with a high-intensity low-energy ion beam is a diffusion process, the dominant parameters for the nitrated zone formation are time, diffusion coefficients, surface sputtering rate and implanted nitrogen ion dose. The two-layer structure of nitrated steel is formed in the saturation regime of the surface layer, the width of which depends on the implanted ion dose and the surface sample temperature. The numerical modeling results agree with the experiments on 40X steel nitriding and allow to predict the structure of surface layers when the geometry system and parameters of high-intensity low-energy nitrogen ion beam are changed.

Acknowledgements

The work was supported by the Russian Science Foundation (Grant No. 17-19-01169).

References

- [1] Totten G E, Funatani K and Xie L 2004 *Handbook of Metallurgical Process Design* (NY: CRC Press) p 284
- [2] Pant P, Dahlmann P, Schlump W and Stein G 1987 *Steel research* **58** 18
- [3] Wei R 1996 *Surf. Coat. Technol.* **83** 218
- [4] Goncharenko I I, Grigoriev S V, Lopatin I V and Koval N N 2003 *Surf. Coat. Technol.* V. **169–170** 419
- [5] Anishchik V M and Uglov V V 2003 *Modification of instrumental materials by ion and plasma beams* (Minsk: Publishing House of the Belarusian State University) p 191
- [6] Ryabchikov A I, Ananin P S, Dektyarev S V, Sivin D O and Shevelev A E 2017 *Vacuum* **143** 447
- [7] Berlin EV, Koval NN and Seidman LA 2012 (Moscow: Technosphere) p 462
- [8] Sun Y and Bell T 1997 *Mater. Sci. and Eng. A* **224** 33
- [9] Hosseini S R, Ashrafizadeh F and Kermanpur A 2010 *Iranian Journal of Science & Technology, Transaction B: Engineering* **34** 553 (Printed in The Islamic Republic of Iran)
- [10] Lopatin I V, Akhmadeev Yu H and Koval N N 2015 *Rev. Sci. Instrum.* **86** 103301